

RFS: REINFORCEMENT LEARNING WITH RESIDUAL FLOW STEERING FOR DEXTEROUS MANIPULATION

Entong Su¹, Tyler Westenbroek¹, Anusha Nagabandi², Abhishek Gupta¹

¹University of Washington, Paul G. Allen School of Computer Science & Engineering

²Amazon Frontier AI & Robotics

ABSTRACT

Imitation learning has emerged as an effective approach for bootstrapping sequential decision-making in robotics, achieving strong performance even in high-dimensional dexterous manipulation tasks. Recent behavior cloning methods further leverage expressive generative models, such as diffusion models and flow matching, to represent multimodal action distributions. However, policies pretrained in this manner often exhibit limited generalization and require additional fine-tuning to achieve robust performance at deployment time. Such adaptation must preserve the global exploration benefits of pretraining while enabling rapid correction of local execution errors. We propose Residual Flow Steering (RFS), a data-efficient reinforcement learning framework for adapting pretrained generative policies. RFS steers a pretrained flow-matching policy by jointly optimizing a residual action and a latent noise distribution, enabling complementary forms of exploration: local refinement through residual corrections and global exploration through latent-space modulation. This design allows efficient adaptation while retaining the expressive structure of the pretrained policy. We demonstrate the effectiveness of RFS on dexterous manipulation tasks, showing efficient fine-tuning both in simulation and in real-world settings when adapting pretrained base policies. Project website: <https://weirdlabuw.github.io/rfs/>

1 INTRODUCTION

Imitation learning from human demonstrations has proven effective for learning high-performing policies in robotics and sequential decision making (Zhao et al., 2023; 2025; Chi et al., 2023; Hussein et al., 2017; Ho and Ermon, 2016). Recent progress has been driven by *generative* imitation learning, which leverages expressive generative models such as diffusion models (Ho et al., 2020) and flow models (Lipman et al., 2022) to capture the distribution of human demonstrations. These approaches are particularly well suited to the inherent multimodality of human behavior (Chi et al., 2023; Black et al., 2024), enabling robust empirical scaling to complex manipulation tasks (Team et al., 2025). However, imitation learning alone often fails to generalize to all test-time scenarios (Team et al., 2025), leaving substantial headroom for policy improvement through test-time fine-tuning toward production-level performance.

While supervised fine-tuning (Ouyang et al., 2022; Black et al., 2024) has proven effective for decision-making systems, it depends on high-quality, curated expert data. Instead, we seek methods that avoid this dependency by leveraging cheaper, suboptimal, or self-collected data. Reinforcement learning (RL) and offline reinforcement learning (offline RL) (Levine et al., 2020) provide a principled framework for behavior improvement, as agents optimize reward objectives rather than relying on expert demonstrations. Although many methods have been proposed to combine imitation learning pretraining with reinforcement learning fine-tuning (Rajeswaran et al., 2018a; Hu et al., 2024; Nair et al., 2018; Nakamoto et al., 2024), these approaches typically rely on closed-form likelihoods (Lillicrap et al., 2015) and reparameterization (Wang et al., 2019), making them incompatible with expressive generative architectures such as diffusion and flow models. Moreover, a key challenge in this setting is balancing adaptation to new tasks with the preservation of knowledge acquired during pretraining.

We begin by viewing residual RL and diffusion steering as instances of a broader class of *policy-modulation* methods, which adapt pretrained generative imitation-learning policies by modulating their inputs or outputs rather than updating model parameters. Residual policy learning (Ankile et al., 2024b) enables local action refinements but struggles to induce global behavioral changes, whereas diffusion steering (Wagenmaker et al., 2025) allows global modulation but offers limited fine-grained control in off-distribution states. These complementary limitations motivate a unified perspective. Motivated by this perspective, we introduce *Residual Flow Steering (RFS)*, a policy-modulation framework for adapting pretrained generative policies using reinforcement learning. RFS jointly modulates the initial latent noise and applies an affine residual correction to the policy output, enabling global semantic adaptation alongside local dexterous refinement.

We instantiate RFS for multi-finger manipulation, developing controllers that achieve robust multi-object grasping in simulation and transfer effectively to the real world. These controllers can be further improved using limited human demonstrations, enabling data-efficient adaptation to real-world dynamics while preserving precision and dexterity. The contributions of this work are: (1) We introduce *residual flow steering* (RFS), an efficient framework for adapting pretrained flow-matching policies. (2) RFS enables effective simulation pretraining from human demonstrations, capturing complex multi-finger coordination behaviors. (3) RFS supports real-world fine-tuning via offline reinforcement learning, outperforming bootstrapped imitation-learning baselines. (4) We conduct extensive ablations to identify the key components of RFS in both simulation and real-world settings.

2 RELATED WORK

Reinforcement Learning with Demonstrations. Imitation learning (IL) is commonly used to bootstrap reinforcement learning (RL) for complex robotic tasks by constraining early exploration and providing strong initial behaviors. Prior work incorporates demonstrations via imitation losses, replay buffers, or reset strategies (Nair et al., 2018; Qin et al., 2022; Xiao et al., 2025a; Hu et al., 2024), while other approaches combine demonstration data with online rollouts to improve exploration efficiency (Ball et al., 2023; Hester et al., 2017; Ankile et al., 2025; Song et al., 2023). Demonstration-guided RL has also been applied to high-DoF dexterous manipulation (Rajeswaran et al., 2018b; Haldar et al., 2023; Wang et al., 2024), demonstrating that while demonstrations accelerate learning, they remain insufficient for achieving the fine-grained precision required in challenging dexterous tasks.

Offline-to-online fine-tuning. Offline-to-online fine-tuning is widely used to improve sample efficiency in robotic RL: a policy is first pretrained on demonstrations and then refined with limited interaction. Lightweight offline-to-online methods (Kostrikov et al., 2021; Nair et al., 2021; Nakamoto et al., 2024) are popular; however, because they operate directly in action space, they often struggle with distribution shift and the fine-grained corrections required for dexterous control. Recent work applies RL to diffusion policies (Ren et al., 2024b; Fang et al., 2025; Davey and Zheng, 2025) and flow-matching policies (Zhang et al., 2025b; McAllister et al., 2025; Park et al., 2025); however, the iterative refinement structure of generative models and the high dimensionality of action-chunked policies make stable RL fine-tuning particularly challenging and prone to instability.

Policy Modulation. Policy modulation methods adapt pretrained policies by modifying either their outputs or their inputs. Output modulation adjusts a base policy’s actions using residual policies (Ankile et al., 2024a; Zeng et al., 2020; Silver et al., 2019; Alakuijala et al., 2021; Davchev et al., 2022; Carvalho et al., 2022; Yuan et al., 2024; Xiao et al., 2025b), enabling effective local corrections but unable to induce global behavioral changes when the base policy is limited. Input modulation methods, such as DSRL (Wagenmaker et al., 2025), instead adjust the latent noise of diffusion policies to modify high-level behavior; however, they remain constrained to the demonstration manifold, limiting off-manifold exploration and fine-grained refinement.

3 BACKGROUND

3.1 FLOW MATCHING

Flow matching (Lipman et al., 2023; Liu, 2022) is a generative modeling framework that learns a time-dependent velocity field that transports a base distribution p_0 to a target distribution p_1 . A

sample evolves according to the ODE $\frac{dx_t}{dt} = v_\theta(x_t, t)$, and the objective is to align the pushforward of p_0 with p_1 while avoiding ODE backpropagation and likelihood computation by supervising conditional paths rather than full marginals (Lipman et al., 2023). Training draws $(x_0, x_1) \sim p_0 \times p_1$, samples $t \sim \mathcal{U}[0, 1]$, forms the interpolation $x_t = (1-t)x_0 + tx_1$, and regresses the predicted velocity toward the straight-path target $v^*(x_t, t) = x_1 - x_0$:

$$\mathcal{L}(\theta) = \mathbb{E}_{x_0 \sim p_0, x_1 \sim p_1, t \sim \mathcal{U}[0, 1]} \|v_\theta(x_t, t) - v^*(x_t, t)\|^2. \quad (1)$$

Given a trained velocity field v_θ , samples from p_1 are obtained via Euler integration (Lipman et al., 2023), yielding a straightforward sampling path:

$$x^{k+1} = x^k + \Delta t_k v_\theta(x^k, t_k), \quad x^0 \sim p_0, \quad x^K \approx x_1. \quad (2)$$

The framework becomes conditional by learning $v_\theta(x_t, t, c)$ with an external variable c . In our setting, an expert dataset $\mathcal{D} = \{s_i, a_i\}$ is used to train a conditional policy velocity field. The corresponding training objective (Eq. 3) learns a conditional velocity field $v_\theta(a_t, t, s)$:

$$\mathcal{L}(\theta) = \mathbb{E}_{a_0 \sim p_0, (s, a) \sim \mathcal{D}, t \sim \mathcal{U}[0, 1]} \|v_\theta(a_t, t, s) - (a - a_0)\|^2, \quad a_t = (1-t)a_0 + ta. \quad (3)$$

Integrating the learned field $v_\theta(a_t, t, s)$ (Eq. 2) produces actions from the policy, enabling expressive multimodal behavior while providing natural control points for downstream adaptation. For notational convenience, we use π_θ and v_θ interchangeably for flow-based policies.

3.2 REINFORCEMENT LEARNING

For adaptation with reinforcement learning (RL), we consider a Markov decision process (MDP) $\mathcal{M} = (\mathcal{S}, \mathcal{A}, \mathcal{T}, r, \gamma)$, where \mathcal{S} and \mathcal{A} denote the state and action spaces, $\mathcal{T}(s' | s, a)$ is the transition kernel, r is the reward function, and $\gamma \in [0, 1]$ is the discount factor. The goal is to learn a stochastic policy $\pi_\theta(a | s)$ that maximizes the expected discounted return $J(\theta) = \mathbb{E}_{\tau \sim p_\pi} [\sum_{t=0}^{\infty} \gamma^t r(s_t, a_t)]$. The choice of RL algorithm is not central to our method; instead, we focus on two policy-modulation paradigms that underlie our approach.

Output modulation. A central example is *residual reinforcement learning*, in which a small residual policy $\pi_r(a | s)$ is trained via RL to correct errors in a pretrained base policy $\pi_\theta(a | s)$ (Ankile et al., 2024b; Silver et al., 2019). Action execution is modified via an additive correction, as shown in Eq. 4.

Input modulation. A complementary line of work modulates the *inputs* to generative policies. Diffusion steering (Wagenmaker et al., 2025) adapts pretrained diffusion models by learning a policy over the initial latent noise rather than sampling it from a fixed Gaussian. Action generation is performed by integrating the flow-matching dynamics in Eq. 2, which maps an initial latent noise a_0 to an action via a denoising process. Diffusion steering optimizes Eq. 5 by adjusting a_0 to steer the generative model’s behavior through this denoising process.

$$\max_{\pi_r} \mathbb{E}_{\substack{s_0 \sim p_0(s), s' \sim p(s'|s, a) \\ a = a_r + a_b, a_r \sim \pi_r(a|s), a_b \sim \pi_\theta(a|s)}} \left[\sum_{t=0}^{\infty} \gamma^t r(s_t, a_t) \right] \quad (4)$$

$$\max_{\pi_{\text{DS}}} \mathbb{E}_{\substack{s_0 \sim p_0(s), s' \sim p(s'|s, a) \\ a_0 \sim \pi_{\text{DS}}(a_0|s), a \sim p_\theta(a|s, a_0)}} \left[\sum_{t=0}^{\infty} \gamma^t r(s_t, a_t) \right] \quad (5)$$

4 RESIDUAL FLOW STEERING: METHOD AND APPLICATIONS

We propose *Residual Flow Steering* (RFS), a unified framework that combines latent-noise steering for global adaptation with residual actions for precise local corrections on top of a pretrained base policy. This formulation enables efficient learning in high-dexterity tasks and supports robust sim-to-real transfer.

4.1 UNIFIED POLICY MODULATION FRAMEWORK

4.1.1 POLICY MODULATION ALGORITHMS FOR ADAPTING PRETRAINED GENERATIVE MODELS

Since residual RL and DSRL represent output and input modulation, respectively, it is natural to view them under a unified policy-modulation perspective. To make this connection explicit, we examine the structure of residual RL (Ankile et al., 2024b; Silver et al., 2019) and latent-noise steering (Wagenmaker et al., 2025; Du and Song, 2025) given a pretrained generative policy $v_\theta(a_t, t, s)$ and a denoising-based sampling function $a \sim \text{Des}(s, a_0, v_\theta)$ with $a_0 \sim \mathcal{N}(0, I)$. We place the two objectives side by side:

$$\max_{\pi_{\text{DS}}} \mathbb{E}_{\substack{s_0 \sim p_0(s) \\ s' \sim p(s'|s, a) \\ a = \text{Des}(s, a_0, v_\theta), \\ a_0 \sim \pi_{\text{DS}}(a_0 | s)}} \left[\sum_{t=0}^{\infty} \gamma^t r(s_t, a_t) \right] \quad \max_{\pi_r} \mathbb{E}_{\substack{s_0 \sim p_0(s) \\ s' \sim p(s'|s, a) \\ a = a_r + a_b, a_r \sim \pi_r(a | s) \\ a_b = \text{Des}(s, a_0, v_\theta), \\ a_0 \sim \mathcal{N}(0, I)}} \left[\sum_{t=0}^{\infty} \gamma^t r(s_t, a_t) \right] \quad (7)$$

Both objectives modulate the behavior of the base policy v_θ —either by adjusting the latent noise or applying an affine action correction. More generally, policy modulation for a generative policy $v_\theta(a_t, t, s)$ optimizes parametric input (g) or output (f) transformations without modifying the underlying parameters θ as formalized in Eq. 8.

4.1.2 RESIDUAL FLOW STEERING FOR JOINT LOCAL AND GLOBAL ADAPTATION

We instantiate the modulation functions f and g as *Residual Flow Steering* (RFS), which unifies residual RL for **output modulation** (Silver et al., 2019; Zhang et al., 2020) with diffusion-steering RL for **input modulation** (Wagenmaker et al., 2025). Input modulation adjusts the latent noise of a flow-matching policy for *global* behavioral variation via $a_0 = \pi_H(a_0 | s)$, while output modulation applies *local* refinements through the affine correction $a = \text{Des}(s, a_0, v_\theta) + a_r$ with $a_r \sim \pi_r(a | s)$. RFS combines these mechanisms through a unified modulation policy $\pi_{\text{RFS}}(a_0, a_r | s)$, jointly producing a_0 for global steering and a_r for precise local adjustments. Here, a_0 shapes the generative model’s overall behavior, while a_r compensates for off-manifold requirements or imperfections in the base policy v_θ . The resulting objective in Eq. 8 is compatible with standard RL algorithms, and the next subsection instantiates RFS for dexterous manipulation in simulation and the real world.

$$\max_{\phi} \mathbb{E}_{\substack{s_0 \sim p_0(s), s' \sim p(s'|s, a) \\ a = f_\phi(a_b, s), a_0 = g_\phi(s) \\ a_b \sim \text{Des}(s, a_0, v_\theta)}} \left[\sum_{t=0}^{\infty} \gamma^t r(s_t, a_t) \right] \quad \max_{\pi_{\text{RFS}}} \mathbb{E}_{\substack{s_0 \sim p_0(s), s' \sim p(s'|s, a) \\ a_0, a_r \sim \pi_{\text{RFS}}(a_0, a_r | s) \\ a_b \sim \text{Des}(s, a_0, v_\theta) \\ a = a_r + a_b}} \left[\sum_{t=0}^{\infty} \gamma^t r(s_t, a_t) \right] \quad (8) \quad (9)$$

4.2 INSTANTIATING RFS FOR DEXTEROUS MANIPULATION

We instantiate RFS for dexterous manipulation through a simulation-to-reality pipeline that enables online fine-tuning in simulation and offline fine-tuning using limited real-world data, applied to state- and vision-based flow-matching policies, respectively, enabling broad exploration and data-efficient adaptation (Fig. 2). We demonstrate the approach across several dexterous manipulation tasks.

4.2.1 SIMULATION TRAINING: DATA GENERATION AND ONLINE RL

Dexterous manipulation poses a key challenge in effective exploration over high-dimensional action spaces. We collect a small set of VR-teleoperated demonstrations **entirely in simulation** to train a base generative policy v_θ using a flow-matching objective (Lipman et al., 2022). Although imperfect

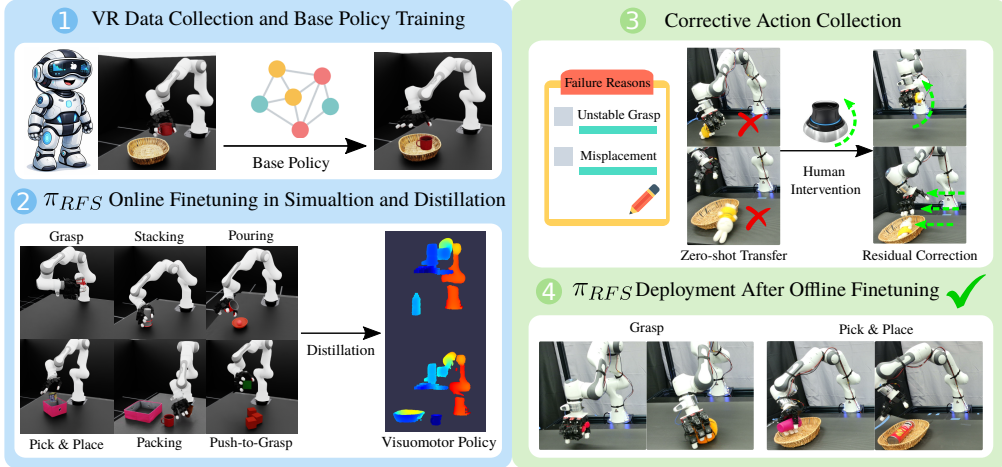


Figure 2: **Overview of the sim-to-real Residual Flow Steering (RFS) pipeline.** (1) VR teleoperation is used to collect demonstrations across multiple manipulation tasks to train task-specific flow-matching base policies. (2) In simulation, the RFS policy π_{RFS} is fine-tuned on top of each base policy and distilled into task-specific visuomotor policies to improve sim-to-real transfer. (3) During zero-shot real-world deployment, human corrective actions correct execution failures such as unstable grasps and misplacement. (4) These corrected transitions are used for offline fine-tuning of π_{RFS} on a Franka–Leap Hand system, improving real-world grasping and pick-and-place performance.

in isolation, this policy captures coordinated hand–arm behaviors and provides a strong initialization for reinforcement learning. We then train the RFS policy π_{RFS} with **online PPO** to optimize grasp success and stability.

The trained RFS policy is used to generate additional simulation demonstrations with access to privileged low-level state information s (e.g., object poses and velocities), which are distilled into point-cloud–conditioned visuomotor policies via a standard student–teacher framework (Chen et al., 2021).

4.2.2 REAL-WORLD FINE-TUNING: OFFLINE RFS

Direct transfer of the distilled visuomotor policy $v_\phi(a_t, o_{\text{pc}}, s_{\text{pro}}, t)$ to the real world often fails under novel objects or varied initial conditions. To bridge this gap, we apply an *offline* RFS fine-tuning stage using a small human-corrected dataset. During data collection, the base policy executes rollouts while a human provides corrective actions at visited states, yielding $\mathcal{D} = \{((o, s), (a_{\text{human}}, a_b, a_0), (o', s'), r)\}$. Residual actions are defined as $a_r = a_{\text{human}} - a_b$, producing the RFS-ready dataset $\mathcal{D}_{\text{RFS}} = \{((o, s), (a_0, a_r), (o', s'), r)\}$. We then train $\pi_{\text{RFS}}(a_0, a_r \mid o_{\text{pc}}, s_{\text{pro}})$ with offline reinforcement learning (Levine et al., 2020), using TD3+BC (Fujimoto and Gu, 2021) for actor–critic updates with imitation regularization.

Critic Update. Given \mathcal{D}_{RFS} , we apply a standard TD-learning critic update in Eq. 10. The critic is conditioned on the combined actions a and a' rather than the decomposed components (a_0, a_r) ; Section 5.2 provides an empirical justification for this design choice.

$$\min_{\phi} \mathbb{E}_{\substack{((o, s), (a_0, a_r), (o', s'), r) \sim \mathcal{D}_{\text{RFS}} \\ a'_0, a'_r \sim \pi_{\text{RFS}}(\cdot | o', s') \\ a_b \sim \text{Push}(o, s, a_0, v_\phi), a = a_b + a_r \\ a'_b \sim \text{Push}(o', s', a'_0, v_\phi), a' = a'_b + a'_r}} [\|Q_\phi(o, s, a) - r - \gamma Q_{\bar{\phi}}(o', s', a')\|^2]. \quad (10)$$

Actor Update. Following TD3+BC (Fujimoto and Gu, 2021), the actor maximizes the critic while applying a BC regularizer on the residual actions:

$$\arg \max_{\pi_{\text{RFS}}} \mathbb{E}_{\substack{((o, s), (a_0, a_r), (o', s'), r) \sim \mathcal{D}_{\text{RFS}} \\ \hat{a}_0, \hat{a}_r \sim \pi_{\text{RFS}}(\cdot | o, s) \\ \hat{a}_b \sim \text{Push}(o, s, \hat{a}_0, v_\phi), \hat{a} = \hat{a}_b + \hat{a}_r}} [Q(o, s, \hat{a}) - \lambda_{\text{BC}} \|\hat{a}_r - a_r\|^2]. \quad (11)$$

5 EXPERIMENTS

We structure our experiments around the following research questions: **Q1**: Does residual refinement improve success in dexterous manipulation tasks in simulation? **Q2**: Which design choices are most effective across both simulation and real-world settings? **Q3**: How does latent-noise modulation influence real-world adaptation performance? As outlined in Section 4.2, we first evaluate RFS for simulation data generation and then for real-world fine-tuning. Our experiments focus primarily on dexterous grasping with a multifingered hand, though the method generalizes to broader manipulation tasks.

5.1 RFS FOR SIMULATION DATA GENERATION AND ONLINE RL TRAINING

5.1.1 SETUP

We evaluate RFS on six simulated tasks: grasping, pick-and-place, non-prehensile push-to-grasp, long-horizon packing, and high-precision stacking and pouring (Fig. 4). Using Apple Vision Pro AR, we collect approximately 400 demonstrations per task and pre-train a generative base policy $v_\theta(a_t, t, s)$ using flow matching (Lipman et al., 2022). Base-policy success rates are reported in Table 1. Although the pretrained policy achieves only moderate success, it provides strong motion priors that RFS further refines via PPO (Schulman et al., 2017b) (Sec. 4.2.1).

5.1.2 BASELINES AND ABLATIONS

Baselines. We compare RFS against a broad suite of reinforcement-learning baselines commonly used for simulation-driven dexterous manipulation. All demonstration-based baselines use the same offline data as RFS. We group these methods into four categories based on their underlying adaptation strategies: **(1) Diffusion/Flow RL Fine-tuning.** DPPO (Ren et al., 2024a) and ReinFlow (Zhang et al., 2025a), which fine-tune demonstration-pretrained diffusion or flow-matching policies through reinforcement learning with environment interaction. **(2) Offline-to-Online RL.** IQL (Kostrikov et al., 2021), AWAC (Nair et al., 2021), and Flow Q-Learning (Park et al., 2025), which are initialized from offline demonstrations and subsequently improved via online interaction. **(3) RL with Demonstrations.** RLPD (Ball et al., 2023) and IBRL (Hu et al., 2024), which incorporate demonstration data directly into policy updates.

Ablations. To isolate the contributions of *both* residual refinement and latent-noise steering, we conduct targeted ablations. (1) **DSRL** (Wagenmaker et al., 2025): steering the latent noise of the base policy *without* residual actions. (2) **State-of-the-Art Residual RL**: strong residual-learning baselines, including Policy Decorator (Yuan et al., 2024) and ResiP (Ankile et al., 2024a).

5.1.3 EMPIRICAL RESULTS IN SIMULATION

Comparison to Baselines: We summarize the performance of all baselines in Table 1 and analyze their behavior as follows:

(1) Diffusion-/Flow-Based RL Fine-Tuning. DPPO (Ren et al., 2024a) underperforms across all tasks, with all success rates below 0.50. ReinFlow Zhang et al. (2025a) shows modest improvements (0.58 grasp, 0.46 pick & place, 0.39 packing), but fails on push-to-grasp, stacking, and pouring. In contrast, restricting RL updates to the initial noise and residual terms (RFS) yields more stable learning, achieving success rates at least 0.35 higher across all tasks than applying RL over the full denoising trajectory.

(2) Offline-to-Online RL. IQL (Kostrikov et al., 2021) is the strongest offline-to-online baseline (0.69 grasp, 0.56 pick-and-place, 0.63 stack, 0.59 pour), but struggles on packing (0.20) and push-to-grasp (0.26). AWAC (Nair et al., 2021) and FlowQ (Park et al., 2025) collapse on multiple tasks.



Figure 3: Simulation and real objects used for dexterous grasping and pick & place.

Overall, offline-to-online RL methods lack directed exploration, whereas RFS leverages base-policy pretraining to achieve consistently higher success rates across all tasks.

(3) **RL with Demonstrations.** RLPD (Ball et al., 2023) performs well on grasping (0.54) and pick-and-place (0.76), but collapses on tasks requiring long-horizon reasoning (e.g., packing) or high-precision manipulation (e.g., stacking and pouring). IBRL (Hu et al., 2024) succeeds only on grasping, packing, and pouring. In contrast, RFS consistently improves over the base policy across all tasks.

Comparison to Ablations. We additionally evaluate strong ablations and related adaptation strategies (Table 1).

(1) **Residual RL methods.** Policy Decorator (Yuan et al., 2024) and ResiP (Ankile et al., 2024a) outperform earlier baselines, but their gains remain largely local, achieving moderate success on grasping (~ 0.60) and pick-and-place (~ 0.50). Performance degrades on sequential and high-precision tasks, including packing (0.40), push-to-grasp (0.15), stacking (0.30), and pouring (0.20). In contrast, RFS achieves ~ 0.80 success on packing and push-to-grasp and ~ 0.90 on the remaining tasks.

(2) **DSRL (Wagenmaker et al., 2025).** DSRL is the strongest baseline, achieving 0.74 (grasp), 0.70 (pick-and-place), 0.64 (packing), and 0.43 (push-to-grasp), but only 0.15 on stacking and 0.26 on pouring. Because its corrections are constrained to the demonstration distribution, DSRL struggles to adapt to challenging or out-of-distribution states.

Overall By jointly modulating the input and output of the base policy, RFS preserves base-policy performance while consistently improving upon it, achieving the highest success rates across all tasks: 0.89 (Grasping), 0.94 (Pick & Place), 0.78 (Packing), 0.72 (Push-to-Grasp), 0.95 (Stacking), and 0.87 (Pouring), with an average success rate of 0.87.

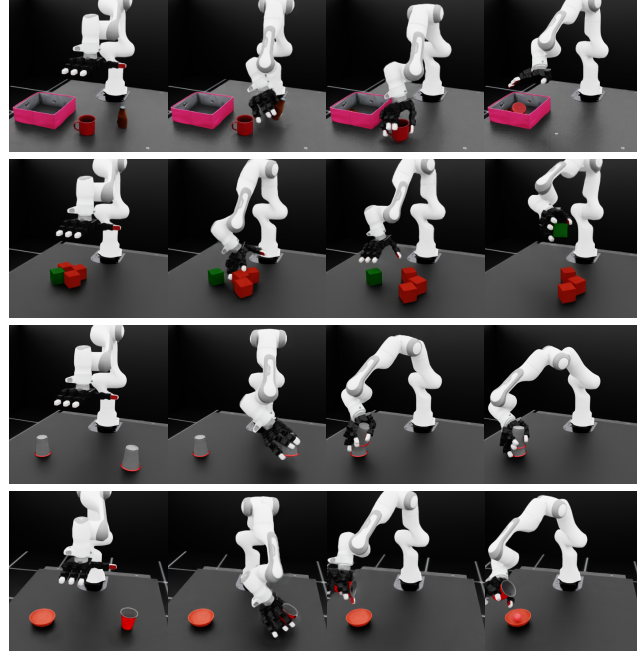


Figure 4: Representative rollouts for the dexterous manipulation tasks. From top to bottom: Packing, Push-to-Grasp, Packing and Stacking.

Category	Method	Grasping	Pick & Place	Packing	Push-to-Grasp	Stacking	Pouring	Avg
Base Policy	Flow Matching (Lipman et al., 2022)	0.495	0.367	0.30	0.131	0.06	0.15	0.250
Diffusion / Flow RL Finetuning	DPPG (Ren et al., 2024a) ReinFlow (Zhang et al., 2025a)	0.41 \pm 0.05 0.584 \pm 0.043	0.433 \pm 0.102 0.462 \pm 0.081	0.186 \pm 0.023 0.100 \pm 0.089	0.04 \pm 0.036 0.398 \pm 0.236	0.00 \pm 0.00 0.59 \pm 0.021	0.00 \pm 0.00 0.32 \pm 0.15	0.178 \pm 0.035 0.409 \pm 0.103
Offline-to-Online RL	IOL (Kostrikov et al., 2021) AWAC (Nair et al., 2021) Flow Q-Learning (Park et al., 2025)	0.690 \pm 0.034 0.485 \pm 0.163 0.050 \pm 0.012	0.560 \pm 0.075 0.240 \pm 0.120 0.486 \pm 0.110	0.203 \pm 0.063 0.00 \pm 0.00 0.00 \pm 0.00	0.267 \pm 0.108 0.00 \pm 0.00 0.381 \pm 0.040	0.625 \pm 0.073 0.780 \pm 0.03 0.00 \pm 0.00	0.583 \pm 0.203 0.625 \pm 0.08 0.00 \pm 0.00	0.488 \pm 0.093 0.355 \pm 0.066 0.153 \pm 0.027
RL with Demonstrations	RLPD (Ball et al., 2023) IBRL (Hu et al., 2024)	0.547 \pm 0.056 0.404 \pm 0.216	0.763 \pm 0.059 0.00 \pm 0.00	0.00 \pm 0.00 0.432 \pm 0.150	0.012 \pm 0.024 0.00 \pm 0.00	0.053 \pm 0.13 0.00 \pm 0.00	0.68 \pm 0.13 0.36 \pm 0.10	0.343 \pm 0.067 0.199 \pm 0.078
Residual RL (State-of-the-Art)	Policy Decorator (Yuan et al., 2024) ResiP (Ankile et al., 2024a)	0.52 \pm 0.09 0.65 \pm 0.096	0.314 \pm 0.160 0.57 \pm 0.014	0.535 \pm 0.021 0.302 \pm 0.028	0.176 \pm 0.016 0.165 \pm 0.18	0.00 \pm 0.00 0.67 \pm 0.05	0.17 \pm 0.23 0.24 \pm 0.12	0.286 \pm 0.086 0.433 \pm 0.081
DSRL (Wagenmaker et al., 2025)		0.732 \pm 0.04	0.692 \pm 0.012	0.639 \pm 0.024	0.430 \pm 0.085	0.135 \pm 0.015	0.268 \pm 0.010	0.483 \pm 0.031
RFS (Ours)		0.899 \pm 0.026	0.939 \pm 0.012	0.781 \pm 0.019	0.721 \pm 0.022	0.951 \pm 0.006	0.873 \pm 0.010	0.861 \pm 0.016

Table 1: Success rates across tasks and RL methods.

5.2 REAL-WORLD OFFLINE FINETUNING

Using data generated by RFS in simulation with access to privileged state information, we distill a point cloud-based policy via a standard student-teacher framework (Chen et al., 2021) for real-world deployment.

We then evaluate offline RFS for adapting the distilled policy in real-world grasping and pick-and-place tasks with both seen and unseen objects (Fig. 1, Fig. 3). Experiments are conducted on a Franka arm equipped with a LEAP hand under Cartesian impedance control at 10 Hz. We evaluate seven objects, including two shared with simulation and five novel deformable objects. Compared to rigid simulation assets, real-world objects exhibit varying compliance, contact dynamics, and appearance, introducing a sim-to-real gap that often causes pretrained policies to fail.

For offline RL fine-tuning, we collect 50 human corrective demonstrations using a SpaceMouse (Appendix A.4.1). Rewards are defined programmatically by segmenting and tracking objects with SAM2 (Ravi et al., 2024) and extracting their centroids (Appendix A.4.2).

5.2.1 BASELINES AND ABLATIONS

Baselines. We evaluate RFS with offline RL (Section 4.2.2) as a data-efficient approach for fine-tuning simulation-trained policies. We compare against three adaptation strategies: (1) **Zero-Shot Transfer**, which deploys the distilled simulation policy without fine-tuning; (2) **BC Fine-tuning**, which uses 50 real-world demonstrations to further train the distilled policy via flow matching; (3) **Co-Training**, which fine-tunes the distilled policy by mixing 50 real-world demonstrations with additional simulated rollouts under the flow-matching objective. These comparisons demonstrate that offline RL fine-tuning yields substantially stronger adaptation than standard flow-matching-based updates.

Critic Design Choices: We additionally study alternative critic architectures in the offline-RL setting, comparing: (1) $Q(a_r, o)$, which conditions only on residual actions and observations; (2) $Q([a_r, a_b], o)$, which conditions on both residual and base-policy actions; (3) $Q(a_b + a_r, o)$ (**Ours**), which conditions solely on the final executed action. This isolates the effect of critic input structure on offline-RL stability and performance.

Ablations: We further analyze offline RL using only residual actions (Residual RL) and only latent-noise steering (DSRL) to quantify their individual contributions.

5.3 EMPIRICAL RESULTS IN THE REAL WORLD

Comparison to Supervised Fine-Tuning.

As shown in Fig. 5 and Fig. 6, the zero-shot policy performs poorly, exhibiting translational and rotational offsets, insufficient finger closure during grasping, and mistimed or misplaced actions in pick-and-place, highlighting a significant sim-to-real gap. While co-training substantially improves performance on known objects (83.3% grasping and 60% pick-and-place success), generalization to unseen objects remains limited. The noisy and inconsistent nature of human-collected data introduces instability and rollout failures, underscoring the difficulty of generalizing to novel objects.

Comparison to Variants of Offline RL.

As discussed in Sec. 4.2.2, TD3+BC conditions the critic on the actor’s output, allowing different Q-function parameterizations. Conditioning the critic on either $Q(a_r, o)$ or $Q([a_r, a_b], o)$ fails to produce consistent grasp poses or precise placement, yielding zero success on both grasping and pick-and-place. In contrast, conditioning on the executed action $Q(a_b + a_r, o)$ —used by both Residual RL and

Method	Pick-and-Place	Grasping
0-shot	50.0 ± 0.0	43.3 ± 6.2
Co-training	60.0 ± 0.0	83.3 ± 0.0
BC	40.0 ± 0.0	73.3 ± 0.0
Residual RL	50.0 ± 0.0	80.0 ± 0.0
DSRL	80.0 ± 0.0	70.0 ± 0.3
RFS (Ours)	90.0 ± 0.0	80.0 ± 2.9

Table 2: Performance on **seen objects**. Values report mean success rate with **95% confidence interval** across trials.

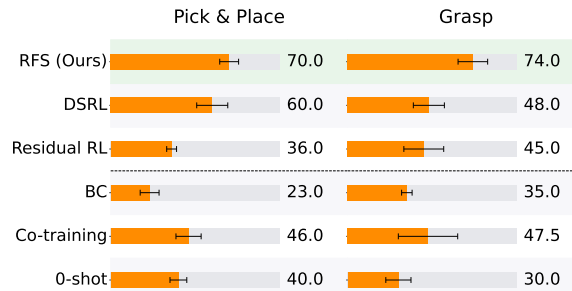


Figure 5: Real-world evaluation results on **unseen objects**. Bars show mean success rates for **Pick-and-Place** (left) and **Grasping** (right), with horizontal error bars denoting the **95% confidence interval**. Numeric annotations report the mean success rate ($\pm 95\% \text{ CI}$).

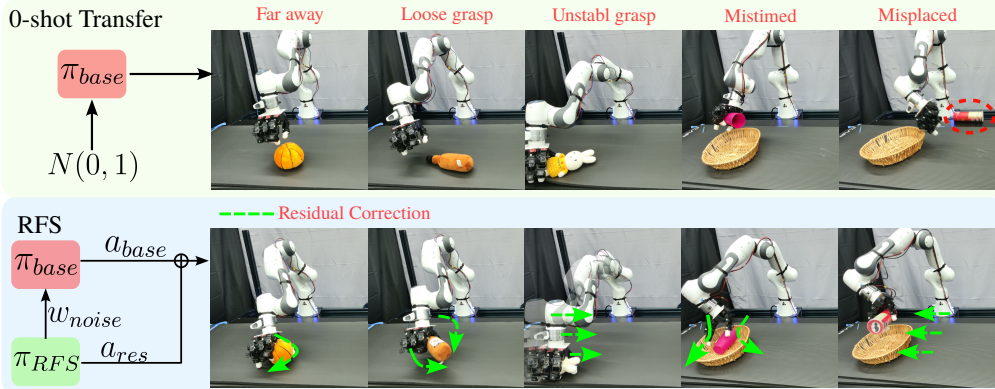


Figure 6: **Common failure modes in real-world manipulation and RFS corrections.** We illustrate five representative failure cases of zero-shot sim-to-real transfer, including early hand closure, loose or unstable grasp poses, and mistimed or misplaced actions during pick-and-place. The top row shows failures produced by the zero-shot policy, while the bottom row shows the corrected outcomes after applying *Residual Flow Steering* (RFS). By jointly correcting action timing, grasp pose, and target location, RFS enables more stable and successful task execution.

RFS (Fig. 5)—achieves substantially higher performance across all baselines. These results indicate that directly coupling residual actions with the executed base actions is critical for stable and effective offline RL adaptation.

Comparison to Ablations of RFS. We evaluate RFS variants that use only residual actions ($\pi(a_r \mid o)$) or only latent-noise steering via DSRL ($\pi(a_0 \mid o)$). As shown in Fig. 5 and Fig. 6, the full model $\pi(a_0, a_r \mid o)$ achieves the strongest performance, particularly on unseen objects in both grasping and pick-and-place tasks. Qualitatively, latent-noise steering facilitates global exploration, while residual actions enable precise local refinement, making their combination more effective than either component alone.

Comparison to Direct Real-Data Fine-Tuning. Fine-tuning RFS on a policy trained solely on real demonstrations yields only modest gains (70% \rightarrow 73% on seen objects and 35% \rightarrow 50% on unseen objects for grasping, with little improvement for pick-and-place), reflecting the limited coverage of the real-data distribution. In contrast, simulation pretraining provides broad coverage over grasps, poses, and perturbations, enabling adaptation behaviors that cannot be learned from real data alone. As a result, fine-tuning a simulation-pretrained policy with a small number of real demonstrations yields substantially larger improvements and stronger generalization.

6 CONCLUSION

We introduced Residual Flow Steering (RFS), a reinforcement learning framework that unifies latent noise steering for global exploration with residual corrections for local refinement. Across both simulation and real-world dexterous manipulation tasks, RFS consistently outperforms conventional baselines—including residual-only methods and diffusion-based steering—by enabling effective simulation pretraining and data-efficient fine-tuning in the real world. Despite these strong results, several limitations remain and point to directions for future work. First, our current implementation primarily relies on point cloud observations, which provide limited semantic and contextual understanding. As a result, performance can degrade in cluttered or semantically rich environments that require higher-level reasoning. Second, real-world adaptation in our framework is currently restricted to offline fine-tuning. This prevents the policy from updating online in response to dynamically changing conditions, limiting its responsiveness and robustness during real-world deployment.

ACKNOWLEDGMENTS

This work was supported by Amazon FAR (Frontier AI & Robotics).

REFERENCES

Minttu Alakuijala, Gabriel Dulac-Arnold, Julien Mairal, Jean Ponce, and Cordelia Schmid. Residual reinforcement learning from demonstrations, 2021. URL <https://arxiv.org/abs/2106.08050>.

Lars Ankile, Anthony Simeonov, Idan Shenfeld, Marcel Torne, and Pulkit Agrawal. From imitation to refinement – residual rl for precise assembly, 2024a. URL <https://arxiv.org/abs/2407.16677>.

Lars Ankile, Anthony Simeonov, Idan Shenfeld, Marcel Torne, and Pulkit Agrawal. From imitation to refinement - residual RL for precise visual assembly. *CoRR*, abs/2407.16677, 2024b. doi: 10.48550/ARXIV.2407.16677. URL <https://doi.org/10.48550/arXiv.2407.16677>.

Lars Ankile, Zhenyu Jiang, Rocky Duan, Guanya Shi, Pieter Abbeel, and Anusha Nagabandi. Residual off-policy rl for finetuning behavior cloning policies, 2025. URL <https://arxiv.org/abs/2509.19301>.

Philip J. Ball, Laura Smith, Ilya Kostrikov, and Sergey Levine. Efficient online reinforcement learning with offline data, 2023. URL <https://arxiv.org/abs/2302.02948>.

Kevin Black, Noah Brown, Danny Driess, Adnan Esmail, Michael Equi, Chelsea Finn, Niccolo Fusai, Lachy Groom, Karol Hausman, Brian Ichter, Szymon Jakubczak, Tim Jones, Liyiming Ke, Sergey Levine, Adrian Li-Bell, Mohith Mothukuri, Suraj Nair, Karl Pertsch, Lucy Xiaoyang Shi, James Tanner, Quan Vuong, Anna Walling, Haohuan Wang, and Ury Zhilinsky. π_0 : A vision-language-action flow model for general robot control. *arXiv preprint arXiv:2410.24164*, 2024. URL <https://arxiv.org/abs/2410.24164>.

Joao Carvalho, Dorothea Koert, Marek Daniv, and Jan Peters. Residual robot learning for object-centric probabilistic movement primitives, 2022. URL <https://arxiv.org/abs/2203.03918>.

Tao Chen, Jie Xu, and Pulkit Agrawal. A system for general in-hand object re-orientation. In Aleksandra Faust, David Hsu, and Gerhard Neumann, editors, *Conference on Robot Learning, 8-11 November 2021, London, UK*, volume 164 of *Proceedings of Machine Learning Research*, pages 297–307. PMLR, 2021. URL <https://proceedings.mlr.press/v164/chen22a.html>.

Cheng Chi, Siyuan Feng, Yilun Du, Zhenjia Xu, Eric Cousineau, Benjamin Burchfiel, and Shuran Song. Diffusion policy: Visuomotor policy learning via action diffusion. In *Proceedings of Robotics: Science and Systems (RSS)*, 2023.

Todor Davchev, Kevin Sebastian Luck, Michael Burke, Franziska Meier, Stefan Schaal, and Subramanian Ramamoorthy. Residual learning from demonstration: Adapting dmpps for contact-rich manipulation. *IEEE Robotics and Automation Letters*, 7(2):4488–4495, April 2022. ISSN 2377-3774. doi: 10.1109/LRA.2022.3150024. URL <http://dx.doi.org/10.1109/LRA.2022.3150024>.

Ashley Davey and Harry Zheng. Convergence of proximal policy gradient method for problems with control dependent diffusion coefficients, 2025. URL <https://arxiv.org/abs/2505.18379>.

Maximilian Du and Shuran Song. Dynaguide: Steering diffusion policies with active dynamic guidance, 2025. URL <https://arxiv.org/abs/2506.13922>.

Linjiajie Fang, Ruoxue Liu, Jing Zhang, Wenjia Wang, and Bing-Yi Jing. Diffusion actor-critic: Formulating constrained policy iteration as diffusion noise regression for offline reinforcement learning, 2025. URL <https://arxiv.org/abs/2405.20555>.

Scott Fujimoto and Shixiang Shane Gu. A minimalist approach to offline reinforcement learning. In *Thirty-Fifth Conference on Neural Information Processing Systems*, 2021.

Siddhant Haldar, Jyothish Pari, Anant Rai, and Lerrel Pinto. Teach a robot to fish: Versatile imitation from one minute of demonstrations, 2023. URL <https://arxiv.org/abs/2303.01497>.

Todd Hester, Matej Vecerik, Olivier Pietquin, Marc Lanctot, Tom Schaul, Bilal Piot, Dan Horgan, John Quan, Andrew Sendonaris, Gabriel Dulac-Arnold, Ian Osband, John Agapiou, Joel Z. Leibo, and Audrunas Gruslys. Deep q-learning from demonstrations, 2017. URL <https://arxiv.org/abs/1704.03732>.

Jonathan Ho and Stefano Ermon. Generative adversarial imitation learning. In *Advances in Neural Information Processing Systems (NeurIPS)*, volume 29, pages 4565–4573, 2016. URL <https://papers.nips.cc/paper/6391-generative-adversarial-imitation-learning>.

Jonathan Ho, Ajay Jain, and Pieter Abbeel. Denoising diffusion probabilistic models. In *Advances in Neural Information Processing Systems (NeurIPS)*, volume 33, pages 6840–6851, 2020. URL <https://arxiv.org/abs/2006.11239>.

Hengyuan Hu, Suvir Mirchandani, and Dorsa Sadigh. Imitation bootstrapped reinforcement learning, 2024. URL <https://arxiv.org/abs/2311.02198>.

Ahmed Hussein, Mohamed Medhat Gaber, Eyad Elyan, and Chrisina Jayne. Imitation learning: A survey of learning methods. *ACM Comput. Surv.*, 50(2), April 2017. ISSN 0360-0300. doi: 10.1145/3054912. URL <https://doi.org/10.1145/3054912>.

Ilya Kostrikov, Ashvin Nair, and Sergey Levine. Offline reinforcement learning with implicit q-learning, 2021. URL <https://arxiv.org/abs/2110.06169>.

Sergey Levine, Aviral Kumar, George Tucker, and Justin Fu. Offline reinforcement learning: Tutorial, review, and perspectives on open problems, 2020. URL <https://arxiv.org/abs/2005.01643>.

Timothy P. Lillicrap, Jonathan J. Hunt, Alexander Pritzel, Nicolas Manfred Otto Heess, Tom Erez, Yuval Tassa, David Silver, and Daan Wierstra. Continuous control with deep reinforcement learning. *CoRR*, abs/1509.02971, 2015. URL <https://api.semanticscholar.org/CorpusID:16326763>.

Yaron Lipman, Ricky T. Q. Chen, Heli Ben-Hamu, Maximilian Nickel, and Matt Le. Flow matching for generative modeling. *arXiv preprint arXiv:2210.02747*, 2022. URL <https://arxiv.org/abs/2210.02747>.

Yaron Lipman, Ricky T. Q. Chen, Heli Ben-Hamu, Maximilian Nickel, and Matt Le. Flow matching for generative modeling, 2023. URL <https://arxiv.org/abs/2210.02747>.

Qiang Liu. Rectified flow: A marginal preserving approach to optimal transport, 2022. URL <https://arxiv.org/abs/2209.14577>.

David McAllister, Songwei Ge, Brent Yi, Chung Min Kim, Ethan Weber, Hongsuk Choi, Haiwen Feng, and Angjoo Kanazawa. Flow matching policy gradients, 2025. URL <https://arxiv.org/abs/2507.21053>.

Mayank Mittal, Calvin Yu, Qinxi Yu, Jingzhou Liu, Nikita Rudin, David Hoeller, Jia Lin Yuan, Ritvik Singh, Yunrong Guo, Hammad Mazhar, Ajay Mandlekar, Buck Babich, Gavriel State, Marco Hutter, and Animesh Garg. Orbit: A unified simulation framework for interactive robot learning environments. *IEEE Robotics and Automation Letters*, 8(6):3740–3747, 2023. doi: 10.1109/LRA.2023.3270034.

Ashvin Nair, Bob McGrew, Marcin Andrychowicz, Wojciech Zaremba, and Pieter Abbeel. Overcoming exploration in reinforcement learning with demonstrations, 2018. URL <https://arxiv.org/abs/1709.10089>.

Ashvin Nair, Abhishek Gupta, Murtaza Dalal, and Sergey Levine. Awac: Accelerating online reinforcement learning with offline datasets, 2021. URL <https://arxiv.org/abs/2006.09359>.

Mitsuhiko Nakamoto, Yuxiang Zhai, Anikait Singh, Max Sobol Mark, Yi Ma, Chelsea Finn, Aviral Kumar, and Sergey Levine. Cal-ql: Calibrated offline rl pre-training for efficient online fine-tuning, 2024. URL <https://arxiv.org/abs/2303.05479>.

NVIDIA, :, Mayank Mittal, Pascal Roth, James Tigue, Antoine Richard, Octi Zhang, Peter Du, Antonio Serrano-Muñoz, Xinjie Yao, René Zurbrügg, Nikita Rudin, Lukasz Wawrzyniak, Milad Rakhsha, Alain Denzler, Eric Heiden, Ales Borovicka, Ossama Ahmed, Iretiayo Akinola, Abrar Anwar, Mark T. Carlson, Ji Yuan Feng, Animesh Garg, Renato Gasoto, Lionel Gulich, Yijie Guo, M. Gussert, Alex Hansen, Mihir Kulkarni, Chenran Li, Wei Liu, Viktor Makoviychuk, Grzegorz Malczyk, Hammad Mazhar, Masoud Moghani, Adithyavairavan Murali, Michael Noseworthy, Alexander Poddubny, Nathan Ratliff, Welf Rehberg, Clemens Schwarke, Ritvik Singh, James Latham Smith, Bingjie Tang, Ruchik Thaker, Matthew Trepte, Karl Van Wyk, Fangzhou Yu, Alex Millane, Vikram Ramasamy, Remo Steiner, Sangeeta Subramanian, Clemens Volk, CY Chen, Neel Jawale, Ashwin Varghese Kuruttukulam, Michael A. Lin, Ajay Mandlekar, Karsten Patzwaldt, John Welsh, Huihua Zhao, Fatima Anes, Jean-Francois Lafleche, Nicolas Moënne-Loccoz, Soowan Park, Rob Stepinski, Dirk Van Gelder, Chris Amevor, Jan Carius, Jumyoung Chang, Anka He Chen, Pablo de Heras Ciechomski, Gilles Daviet, Mohammad Mohajerani, Julia von Muralt, Viktor Reutskyy, Michael Sauter, Simon Schirm, Eric L. Shi, Pierre Terdiman, Kenny Vilella, Tobias Widmer, Gordon Yeoman, Tiffany Chen, Sergey Grizan, Cathy Li, Lotus Li, Connor Smith, Rafael Wiltz, Kostas Alexis, Yan Chang, David Chu, Linxi "Jim" Fan, Farbod Farshidian, Ankur Handa, Spencer Huang, Marco Hutter, Yashraj Narang, Soha Pouya, Shiwei Sheng, Yuke Zhu, Miles Macklin, Adam Moravanszky, Philipp Reist, Yunrong Guo, David Hoeller, and Gavriel State. Isaac lab: A gpu-accelerated simulation framework for multi-modal robot learning, 2025. URL <https://arxiv.org/abs/2511.04831>.

Long Ouyang, Jeff Wu, Xu Jiang, Diogo Almeida, Carroll Wainwright, Pamela Mishkin, Chong Zhang, Sandhini Agarwal, Katarina Slama, Alex Ray, John Schulman, Jacob Hilton, Fraser Kelton, Luke Miller, Maddie Simens, Amanda Askell, Peter Welinder, Paul Christiano, Jan Leike, and Ryan Lowe. Training language models to follow instructions with human feedback. *arXiv preprint arXiv:2203.02155*, 2022. URL <https://arxiv.org/abs/2203.02155>.

Seohong Park, Qiyang Li, and Sergey Levine. Flow q-learning, 2025. URL <https://arxiv.org/abs/2502.02538>.

Younghyo Park and Pulkit Agrawal. Using apple vision pro to train and control robots, 2024. URL <https://github.com/Improbable-AI/VisionProTeleop>.

Charles R. Qi, Hao Su, Kaichun Mo, and Leonidas J. Guibas. Pointnet: Deep learning on point sets for 3d classification and segmentation, 2017. URL <https://arxiv.org/abs/1612.00593>.

Yuzhe Qin, Yueh-Hua Wu, Shaowei Liu, Hanwen Jiang, Ruihan Yang, Yang Fu, and Xiaolong Wang. Dexmv: Imitation learning for dexterous manipulation from human videos, 2022. URL <https://arxiv.org/abs/2108.05877>.

Aravind Rajeswaran, Vikash Kumar, Abhishek Gupta, Giulia Vezzani, John Schulman, Emanuel Todorov, and Sergey Levine. Learning complex dexterous manipulation with deep reinforcement learning and demonstrations, 2018a. URL <https://arxiv.org/abs/1709.10087>.

Aravind Rajeswaran, Vikash Kumar, Abhishek Gupta, Giulia Vezzani, John Schulman, Emanuel Todorov, and Sergey Levine. Learning complex dexterous manipulation with deep reinforcement learning and demonstrations, 2018b. URL <https://arxiv.org/abs/1709.10087>.

Nikhila Ravi, Valentin Gabeur, Yuan-Ting Hu, Ronghang Hu, Chaitanya Ryali, Tengyu Ma, Haitham Khedr, Roman Rädle, Chloe Rolland, Laura Gustafson, Eric Mintun, Junting Pan, Kalyan Vaiduve Alwala, Nicolas Carion, Chao-Yuan Wu, Ross Girshick, Piotr Dollár, and Christoph Feichtenhofer. Sam 2: Segment anything in images and videos. *arXiv preprint arXiv:2408.00714*, 2024. URL <https://arxiv.org/abs/2408.00714>.

Allen Z. Ren, Justin Lidard, Lars L. Ankile, Anthony Simeonov, Pulkit Agrawal, Anirudha Majumdar, Benjamin Burchfiel, Hongkai Dai, and Max Simchowitz. Diffusion policy policy optimization, 2024a. URL <https://arxiv.org/abs/2409.00588>.

Allen Z. Ren, Justin Lidard, Lars L. Ankile, Anthony Simeonov, Pulkit Agrawal, Anirudha Majumdar, Benjamin Burchfiel, Hongkai Dai, and Max Simchowitz. Diffusion policy policy optimization, 2024b. URL <https://arxiv.org/abs/2409.00588>.

John Schulman, Filip Wolski, Prafulla Dhariwal, Alec Radford, and Oleg Klimov. Proximal policy optimization algorithms, 2017a. URL <https://arxiv.org/abs/1707.06347>.

John Schulman, Filip Wolski, Prafulla Dhariwal, Alec Radford, and Oleg Klimov. Proximal policy optimization algorithms, 2017b. URL <https://arxiv.org/abs/1707.06347>.

Tom Silver, Kelsey Allen, Josh Tenenbaum, and Leslie Kaelbling. Residual policy learning, 2019. URL <https://arxiv.org/abs/1812.06298>.

Yuda Song, Yifei Zhou, Ayush Sekhari, J. Andrew Bagnell, Akshay Krishnamurthy, and Wen Sun. Hybrid rl: Using both offline and online data can make rl efficient, 2023. URL <https://arxiv.org/abs/2210.06718>.

TRI LBM Team, Jose Barreiros, Andrew Beaulieu, Aditya Bhat, Rick Cory, Eric Cousineau, Hongkai Dai, Ching-Hsin Fang, Kuniyatsu Hashimoto, Muhammad Zubair Irshad, Masha Itkina, Naveen Kuppuswamy, Kuan-Hui Lee, Katherine Liu, Dale McConachie, Ian McMahon, Haruki Nishimura, Calder Phillips-Grafflin, Charles Richter, Paarth Shah, Krishnan Srinivasan, Blake Wulfe, Chen Xu, Mengchao Zhang, Alex Alspach, Maya Angeles, Kushal Arora, Victor Campagnolo Guizilini, Alejandro Castro, Dian Chen, Ting-Sheng Chu, Sam Creasey, Sean Curtis, Richard Denitto, Emma Dixon, Eric Dusel, Matthew Ferreira, Aimee Goncalves, Grant Gould, Damrong Guoy, Swati Gupta, Xuchen Han, Kyle Hatch, Brendan Hathaway, Allison Henry, Hillel Hochsztain, Phoebe Horgan, Shun Iwase, Donovan Jackson, Siddharth Karamcheti, Sedrick Keh, Joseph Masterjohn, Jean Mercat, Patrick Miller, Paul Mitiguy, Tony Nguyen, Jeremy Nimmer, Yuki Noguchi, Reko Ong, Aykut Onol, Owen Pfannenstiehl, Richard Poyner, Leticia Priebe Mendes Rocha, Gordon Richardson, Christopher Rodriguez, Derick Seale, Michael Sherman, Mariah Smith-Jones, David Tago, Pavel Tokmakov, Matthew Tran, Basile Van Hoorick, Igor Vasiljevic, Sergey Zakharov, Mark Zolotas, Rares Ambrus, and Kerri Fetzer-Borelli. A careful examination of large behavior models for multitask dexterous manipulation. *arXiv preprint arXiv:2507.05331*, 2025. URL <https://arxiv.org/abs/2507.05331>.

Andrew Wagenmaker, Mitsuhiro Nakamoto, Yunchu Zhang, Seohong Park, Waleed Yagoub, Anusha Nagabandi, Abhishek Gupta, and Sergey Levine. Steering your diffusion policy with latent space reinforcement learning, 2025. URL <https://arxiv.org/abs/2506.15799>.

Huan Wang, Stephan Zheng, Caiming Xiong, and Richard Socher. On the generalization gap in reparameterizable reinforcement learning, 2019. URL <https://arxiv.org/abs/1905.12654>.

Jun Wang, Ying Yuan, Haichuan Che, Haozhi Qi, Yi Ma, Jitendra Malik, and Xiaolong Wang. Lessons from learning to spin "pens", 2024. URL <https://arxiv.org/abs/2407.18902>.

Wenli Xiao, Haotian Lin, Andy Peng, Haoru Xue, Tairan He, Yuqi Xie, Fengyuan Hu, Jimmy Wu, Zhengyi Luo, Linxi "Jim" Fan, Guanya Shi, and Yuke Zhu. Self-improving vision-language-action models with data generation via residual rl, 2025a. URL <https://arxiv.org/abs/2511.00091>.

Wenli Xiao, Haotian Lin, Andy Peng, Haoru Xue, Tairan He, Yuqi Xie, Fengyuan Hu, Jimmy Wu, Zhengyi Luo, Linxi "Jim" Fan, Guanya Shi, and Yuke Zhu. Self-improving vision-language-action models with data generation via residual rl, 2025b. URL <https://arxiv.org/abs/2511.00091>.

Xiu Yuan, Tongzhou Mu, Stone Tao, Yunhao Fang, Mengke Zhang, and Hao Su. Policy decorator: Model-agnostic online refinement for large policy model, 2024. URL <https://arxiv.org/abs/2412.13630>.

Andy Zeng, Shuran Song, Johnny Lee, Alberto Rodriguez, and Thomas Funkhouser. Tossingbot: Learning to throw arbitrary objects with residual physics, 2020. URL <https://arxiv.org/abs/1903.11239>.

Shangtong Zhang, Wendelin Boehmer, and Shimon Whiteson. Deep residual reinforcement learning, 2020. URL <https://arxiv.org/abs/1905.01072>.

Tonghe Zhang, Chao Yu, Sichang Su, and Yu Wang. Reinflow: Fine-tuning flow matching policy with online reinforcement learning, 2025a. URL <https://arxiv.org/abs/2505.22094>.

Tonghe Zhang, Chao Yu, Sichang Su, and Yu Wang. Reinflow: Fine-tuning flow matching policy with online reinforcement learning, 2025b. URL <https://arxiv.org/abs/2505.22094>.

Tony Z. Zhao, Vikash Kumar, Sergey Levine, and Chelsea Finn. Learning fine-grained bimanual manipulation with low-cost hardware. In *Proceedings of Robotics: Science and Systems (RSS)*, 2023. URL <https://arxiv.org/abs/2304.13705>. ALOHA: Action Chunking with Transformers (ACT).

Tony Z. Zhao, Jonathan Tompson, Danny Driess, Pete Florence, Seyed Kamyar Seyed Ghasemipour, Chelsea Finn, and Ayzaan Wahid. Aloha unleashed: A simple recipe for robot dexterity. In *Proceedings of The 8th Conference on Robot Learning (CoRL)*, volume 270 of *Proceedings of Machine Learning Research*, pages 1910–1924. PMLR, 2025. URL <https://proceedings.mlr.press/v270/zhao25b.html>.

A APPENDIX

A.1 SIMULATION SETUP AND TRAINING

A.1.1 REINFORCEMENT LEARNING DESIGN CHOICES

To enhance robustness and mitigate controller misalignment for sim-to-real transfer, we introduce the following design choices:

Simulator: All of our simulated tasks are built on IsaacLab (NVIDIA et al., 2025).

Teleoperation: We further developed the teleoperation system in IsaacLab (NVIDIA et al., 2025) to make it more suitable for dexterous hand manipulation.

External Disturbances: Apply random external disturbances to each joint at intervals of 2–5 steps, encouraging the policy to recover from perturbations.

Observation Space: In the simulation RL training, we use state-based information, including the robot proprioception, the current object pose, the target object pose, and binary contact signals between each fingertip and the object.

Data Collection: We use the Vision Pro for data collection, leveraging an application built on IsaacLab Mittal et al. (2023).

A.2 PPO HYPERPARAMETERS

We train the Residual Flow Steering (RFS) policy using Proximal Policy Optimization (PPO) (Schulman et al., 2017a) during online fine-tuning in simulation. The same set of hyperparameters is used across all tasks.

Policy and Value Networks. Both the RFS policy $\pi_{\text{RFS}}(a_0, a_r \mid s)$ and the value function $V(s)$ are parameterized by multilayer perceptrons with three hidden layers of width 256, 128, 64 and ReLU activations. The policy outputs both the latent noise steering variable w_0 for flow matching base policy and the residual action a_r .

Table 3: PPO hyperparameters used for online RFS training in simulation.

Hyperparameter	Value
Discount factor γ	0.99
GAE parameter λ	0.95
Policy learning rate	3×10^{-4}
Value learning rate	1×10^{-3}
Optimizer	Adam
Clip range ϵ	0.2
Value loss coefficient	0.5
Max gradient norm	1.0
Minibatch size	1024

A.2.1 POLICY DISTILLATION

To improve sim-to-real transfer, we use point clouds as visual observations. To mitigate errors from camera calibration and hardware variations, we collect simulation data from multiple camera viewpoints and calibrate all point clouds to the robot base frame. We further inject random noise into the camera extrinsics during data collection and into the point clouds during training to improve robustness. In simulation, we collect 1,000 demonstrations for each of the grasping and pick-and-place tasks to train the policy.

A.3 REAL WORLD EXPERIMENT DETAILS

A.3.1 REAL ROBOT EVALUATION

For real-robot evaluation, we tested our policy within a 30×50 cm region located 0.35–0.65 m from the robot base and spanning -0.25 to 0.25 m horizontally. We evaluated known objects with 20 trials each, and seven unknown objects with 10 trials each.

A.4 TELEOPERATION DATA COLLECTION

For real-world teleoperation data collection in the co-training setup, we developed a Vision Pro application based on Park and Agrawal (2024) that supports teleoperation at a controlled frequency of 10Hz.

A.4.1 OFFLINE DATA COLLECTION

When the hand is within ~ 10 cm of the table—where most failures occur (Fig. 6), we enable human intervention via a SpaceMouse (Fig. 8). Rather than granting full manual control, which would shift the policy distribution, we compute residual corrections as bounded deltas from the base policy output, conditioned on the current observation. Specifically, the CFM module predicts the next action, and we take the difference between this rollout and the operator’s input. Residuals are constrained to ≤ 1.5 cm in Cartesian translation and ≤ 0.05 rad for finger motion, applied uniformly across all joints. In practice, corrections were limited to Cartesian translation and minor finger adjustments, with the SpaceMouse z -axis mapped to finger motion.

A.4.2 REWARD FUNCTION DESIGN

In the real world, the reward is constructed using SAM2 (Ravi et al., 2024) to track the object in image space and extract its point cloud, from which the object center is computed. The reward consists of two terms: (1) the distance between the object center and the palm, obtained via forward kinematics, and (2) the object’s lifting height, which encourages stable grasp execution. Figure 7 illustrates the reward trend.

A.5 TD3+BC HYPERPARAMETERS

We fine-tune the Residual Flow Steering (RFS) policy in the real world using the TD3+BC algorithm (Fujimoto and Gu, 2021), operating in an offline setting with a fixed dataset of human-corrected transitions. Observations are represented as point clouds, and the perception backbone is adapted from PointNet (Qi et al., 2017). The TD3+BC hyperparameters used in all real-world experiments are summarized in Table 4.

Table 4: TD3+BC hyperparameters used for offline RFS fine-tuning in real-world experiments.

Hyperparameter	Value
Actor learning rate	3×10^{-4}
Critic learning rate	3×10^{-4}
Policy update delay	10
Target policy noise std	0.2
Target noise clip	0.5
Behavior cloning weight λ_{BC}	0.2
Batch size	512
Replay buffer	Fixed offline dataset

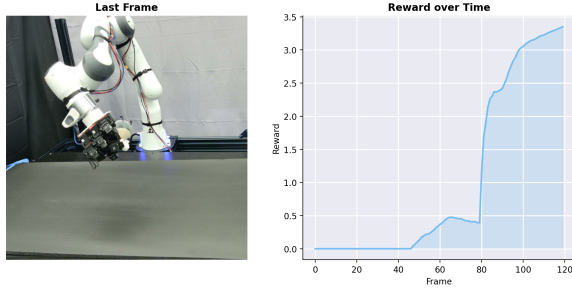


Figure 7: Reward progression over time in real-world experiments.

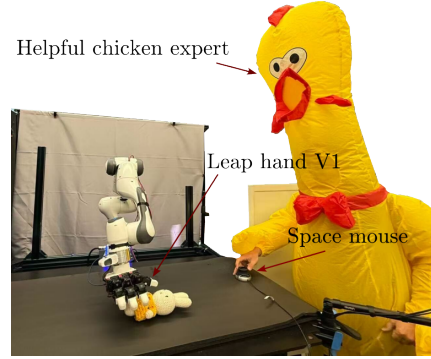


Figure 8: Offline real-world data collection setup using the Leap Hand V1 and a space mouse interface.

B SIMULATION BASELINES AND CODEBASES

We compare RFS against a diverse set of simulation baselines spanning diffusion/flow RL fine-tuning, offline-to-online RL, RL with demonstrations, and the SOTA residual RL methods. For each baseline, we use the open-source implementations and follow their recommended training protocols.

- **DPPO** (Ren et al., 2024a):
<https://github.com/irom-princeton/dppo>
- **ReinFlow** (Zhang et al., 2025a):
<https://github.com/ReinFlow>
- **Flow Q-Learning (FQL) and IQIL** (Park et al., 2025):
<https://github.com/seohongpark/fql/tree/master/agents>
- **AWAC** (Nair et al., 2021):
<https://github.com/ikostrikov/jaxrl>
- **RLPD and IBRL** (Hu et al., 2024):
<https://github.com/hengyuan-hu/ibrl>
- **Policy Decorator** (Yuan et al., 2024):
https://github.com/tongzhoumu/policy_decorator
- **ReSIP** (Ankile et al., 2024a):
<https://github.com/ankile/robust-rearrangement>

All baselines are trained using the same simulator, observation modalities, and task specifications as RFS to ensure a fair comparison.